Optical Phase Conjugation with Gain in a Bulk Semiconductor

David O. Caplan and Prem Kumar

Department of Electrical Engineering and Computer Science
Northwestern University, 2145 N. Sheridan Road
Evanston, Illinois 60208-3118
Phone: (708) 491-4128; Fax: (708) 491-4455

ABSTRACT

We experimentally demonstrate a method of high-speed optical amplification using degenerate four-wave mixing in a bulk semiconductor, CdTe. In our experiment, both transmitted probe and phase-conjugate beams are amplified in accordance with theory. We propose that this approach, which performs optical splitting with gain, can be used with multiple input signals, leading to potential applications including image amplification, information distribution and optical computing.

Keywords: optical amplification, four-wave mixing, FWM, phase-conjugation, semiconductor, nonlinear optics.

1 INTRODUCTION

Four-wave mixing (FWM) is a nonlinear optical process that has been used extensively in applications such as optical amplification,[1,2] frequency conversion,[3,4] and the generation of non-classical light.[5,6] As a source of phase-conjugated or time-reversed waves,[7] FWM can be used to correct for spatial aberrations[8] through wavefront inversion, and temporal aberrations such as dispersion by parametric amplification[9] or spectral inversion.[10,11] These properties have also been applied to areas such as optical signal processing and computing,[12] image transmission,[13,14] and adaptive optics.[8]

Until recently, FWM has been performed predominantly in fibers with weak nonlinearities over long interaction lengths, in highly nonlinear vapors such as Na or K[15] which are difficult to use in a non-laboratory environment, or in photorefractive materials which have very slow (msec) response times. Our FWM experiments are performed in compact readily available semiconductors which feature large nonlinearities, fast (nsec) response times, and ease of fabrication, processing, and integration into working systems.

In Section 2 we review the plane-wave theory of degenerate FWM (DFWM) and then extend the existing analytical solutions for reflected conjugate and transmitted probe beams to account for the Gaussian nature of the laser beams. The experiments are described in Section 3 and present a method of optical splitting with gain through nearly phase-matched forward-FWM in CdTe. We have observed conjugate reflectivities up to 200% corresponding to transmitted probe amplifications of 300%, which is in agreement with the derived theory. Experimental results and comparison with the theory are presented in Section 4.

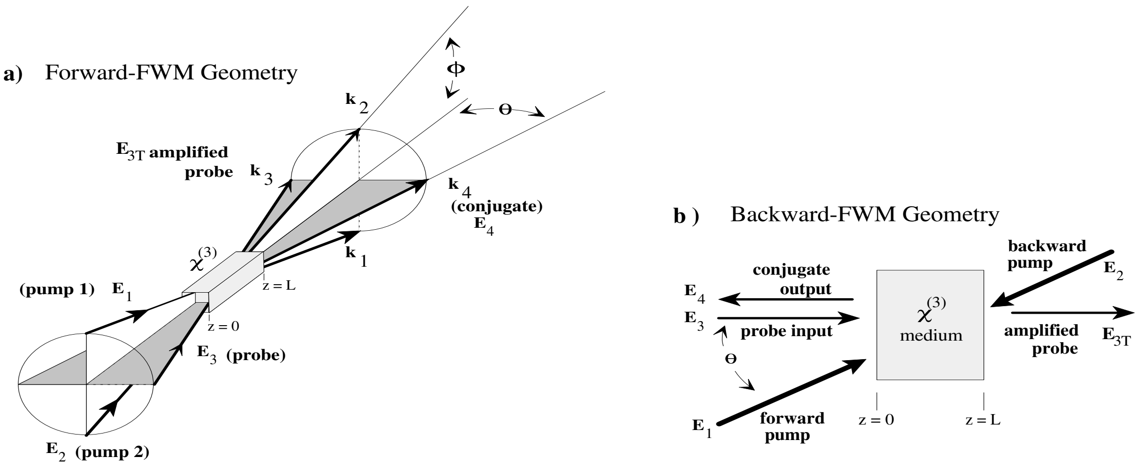

Figure 1: a) Forward and b) backward DFWM geometries.

2 FWM THEORETICAL BACKGROUND

2.1 Review of plane-wave theory

Consider the FWM geometries shown in Figure 1, comprised of two strong pump waves, $\mathbf{E}_1$ and $\mathbf{E}_2$, a weak probe input $\mathbf{E}_3$, and a phase-conjugate output beam $\mathbf{E}_4$. The fields, $\mathbf{E}_i$, are taken to be linearly polarized plane waves of angular frequency ω propagating in direction $\mathbf{k}_i$ at small angles ϕ and θ from the z direction. With the choice of wave vectors shown in Figure 1, phase-matching is achieved when $\mathbf{k}_1 + \mathbf{k}_2 = \mathbf{k}_3 + \mathbf{k}_4$.

For backward-FWM, with counter-propagating pumps, phase-matching occurs when $\mathbf{k}_4 = -\mathbf{k}_3$. In the forward-FWM configuration the z components of the pump beams $\mathbf{E}_1$ and $\mathbf{E}_2$ are co-propagating (i.e., $\mathbf{k}_{z_1} = \mathbf{k}_{z_2}$), but the phase-matching condition remains: $\mathbf{k}_4 = \mathbf{k}_1 + \mathbf{k}_2 - \mathbf{k}_3$. This can only be achieved if $\phi = \theta$, forcing the system to three dimensions. For a given pump angle ϕ, there is an entire cone at angle ϕ w.r.t. the z-axis where input signals $\mathbf{k}_i$ are perfectly phase-matched. Thus, principle, multiple signals could be phase-conjugated simultaneously.

For the nearly phase-matched case, also known as three wave mixing (TWM), the two forward pumps are collinear, propagating along the z-axis. In this case, $\phi = 0 \approx \theta$ minimizing phase-mismatch, and the 3-D system becomes planar (see Figure 2a). For Gaussian beams, which have a distribution of propagation vectors, good phase-matching can be obtained as long as θ is small.

Following the approach in references 1 and 6, the expressions for phase-conjugate reflectivity (R_{pc}) and probe transmission (T_{pc}) can be derived. Based on the usual assumptions of undepleted pumps and slowly-varying-wave-amplitudes in a lossless material, the coefficients for forward FWM are given by

$$R_{\mathrm{pc}} = \left|\frac{\mathbf{E}_4(L)}{\mathbf{E}_3^*(0)}\right|^2 = \sinh^2 \kappa_4 L, \tag{1}$$

$$T_{\mathrm{pc}} = \left|\frac{\mathbf{E}_3(L)}{\mathbf{E}_3(0)}\right|^2 = \cosh^2 \kappa_4 L, \tag{2}$$

$$\kappa_4 = \frac{3\epsilon_o \mu_o \omega^2 \chi^{(3)} \mathbf{E}_1(0)\mathbf{E}_2(0)}{k} = \frac{3\chi^{(3)}\omega I}{2\epsilon_o c^2 n^2}, \tag{3}$$

where κ_4 is the nonlinear coupling constant (in MKS units), $\chi^{(3)}$ is the third-order susceptibility of the nonlinear medium, c is the speed of light in vacuum, n is the linear refractive index, and L is the interaction length. Using the expressions above, a distinct relationship between R and T is established in contrast with the usual equality, $T + R = 1$,

$$T_{\mathrm{pc}} = R_{\mathrm{pc}} + 1. \tag{4}$$

The transmitted wave is always more intense than the incident wave, ($T_{\mathrm{pc}} \geq 1$), and for $\kappa_4 L \geq 0.9$, the reflected intensity exceeds that of the input. In other words, the FWM process can amplify both transmitted and reflected waves, with the additional energy coming from phase-matched scattering of the pump beams in the directions of the probe and conjugate output signals. Figure 2b provides a more intuitive model of the scattering mechanism. The pump beams $\mathbf{E}_{1,2}$, and signal beam $\mathbf{E}_3$ interfere to form fringe patterns which in turn create a real index grating due to the intensity-dependent refractive index of $\chi^{(3)}$ materials. The conjugate beam, $\mathbf{E}_4$, corresponds to the first-order Bragg diffracted transmission of the pump whereas the amplified portion of the transmitted probe, $\mathbf{E}_{3t}$, corresponds to the zeroth-order Bragg reflection.

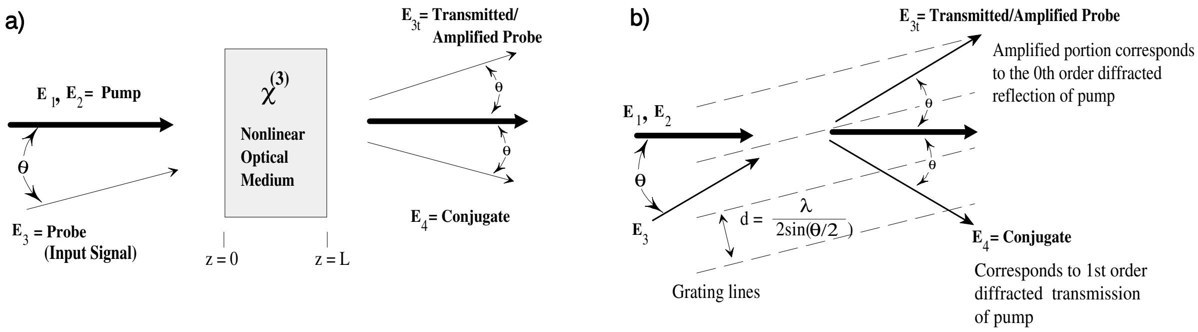

Figure 2: (a) Nearly phase-matched forward FWM geometry, and (b) the forward FWM grating model.

2.2 FWM with Gaussian beams

The above theory neglects the Gaussian nature of the beams since it is based on the plane-wave assumption, i.e., the four interacting waves are infinite plane-waves with uniform intensity profiles. Accounting for the Gaussian spatial profile of the interacting beams significantly impacts the expressions for the phase-conjugate reflectivity R_{pc} and probe transmission T_{pc} as shown below.

By adding the Gaussian transverse spatial dependence, the equations for the input and conjugate fields $\mathbf{E}_3$ and $\mathbf{E}_4$ become (neglecting the constant phase terms):

$$\mathbf{E}_3(\rho, z) = \mathbf{E}_3(z)\exp(-\frac{\rho^2}{2a^2}), \tag{5}$$

$$\mathbf{E}_4(\rho, z) = \mathbf{E}_3^*(z)\exp(-\frac{\rho^2}{2a^2})\sinh(\kappa_5 I(0)\exp(-\frac{\rho^2}{a^2})), \tag{6}$$

$$\kappa_5 = \frac{3\chi^{(3)}\omega L}{2\epsilon_o c^2 n^2}, \tag{7}$$

and the conjugate reflectivity becomes,

$$R^g_{\rm pc} = \frac{\int_0^\infty |\mathbf{E}_4(\rho,0)|^2 \rho d\rho}{\int_0^\infty |\mathbf{E}_3(\rho,0)|^2 \rho d\rho} = \frac{\sinh(2\kappa_5 I(0))}{4\kappa_5 I(0)} - \tfrac{1}{2}. \tag{8}$$

Using the same approach to solve for the transmission coefficient, we obtain:

$$T^g_{\rm pc} = \frac{\sinh(2\kappa_5 I(0))}{4\kappa_5 I(0)} + \tfrac{1}{2}. \tag{9}$$

Similarly for backward FWM, the reflection and transmission coefficients become:

$$R_{\rm pc} = \tan^2 \kappa_4 L \qquad \longrightarrow \qquad R^g_{\rm pc} = \frac{\tan(\kappa_5 I(0))}{\kappa_5 I(0)} - 1 \tag{10}$$

$$T_{\rm pc} = \sec^2 \kappa_4 L \qquad \longrightarrow \qquad T^g_{\rm pc} = \frac{\tan(\kappa_5 I(0))}{\kappa_5 I(0)}. \tag{11}$$

From Eqs. 8 - 11, the $T_{\rm pc} = R_{\rm pc} + 1$ relationship for plane-waves is clearly maintained for Gaussian beams, in both forward and backward FWM configurations.

The effects of the Gaussian profile on conjugate reflectivity can be seen in Figure 3 with both forward and backward cases shown together for comparison. Conjugate reflectivity is quadratic for both plane-waves and Gaussian beams for small values of the argument $\kappa_5 I(0)$, however the Gaussian case is smaller by a factor of 1/3.

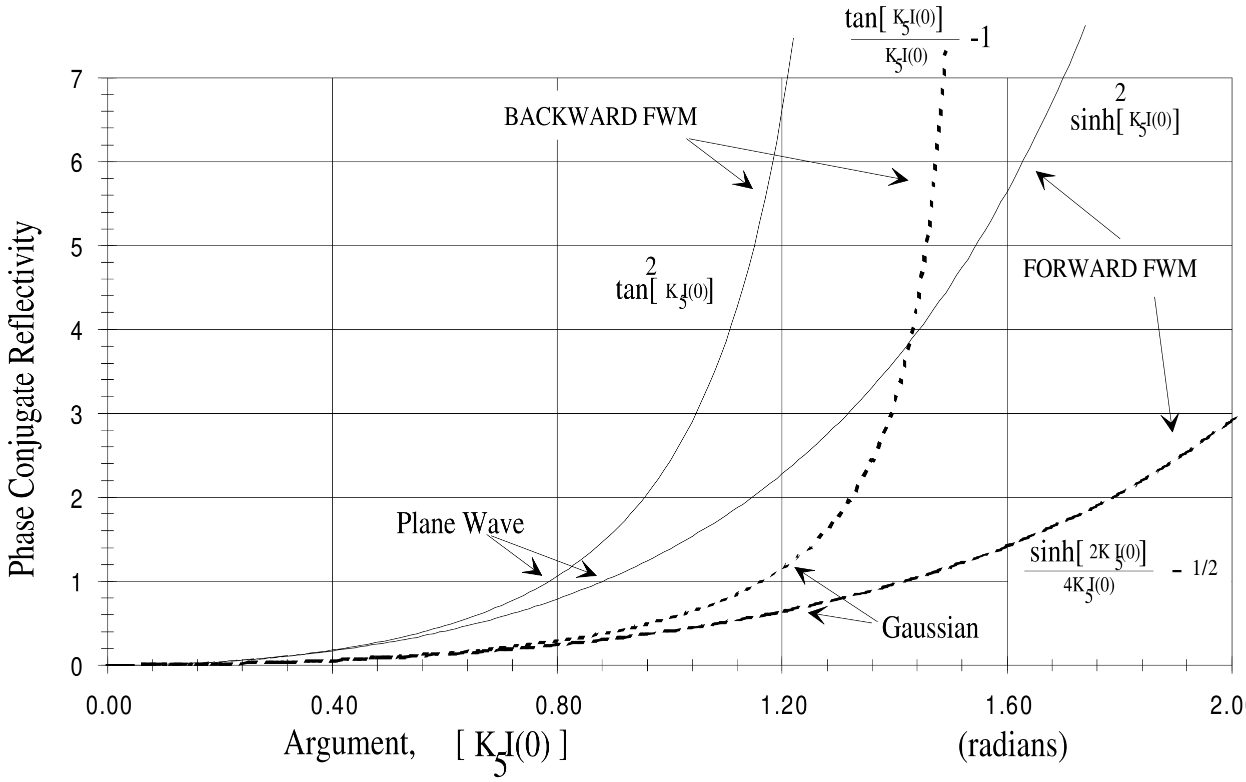

Figure 3: Comparison of plane-wave -vs- Gaussian and forward -vs- backward phase-conjugate reflectivity trends as a function of varying intensity, with $\kappa_5 I(0) < 2.0$ radians, (115 degrees).

In backward FWM, the Gaussian reflectivity tends to vary as $\tan[\kappa_5 I(0)]$ for larger values of $\kappa_5 I(0)$, and accordingly, is approximately equal to the square root of the plane-wave reflectivity. As in the plane-wave case, however, infinite conjugate reflectivity can still be theoretically achieved as the argument approaches $\pi/2$. It should be noted that the above derivations do not account for the effects of gain-induced diffraction (GID),[16] and therefore, are most accurate in the limits of small gains, ($R_{\mathrm{pc}} \sim 1$). Initial FWM experiments in CS_2, which has a well characterized nonlinearity, support these derivations, as seen by the excellent match between the theoretical Gaussian and experimental conjugate reflectivities shown in Figure 4.

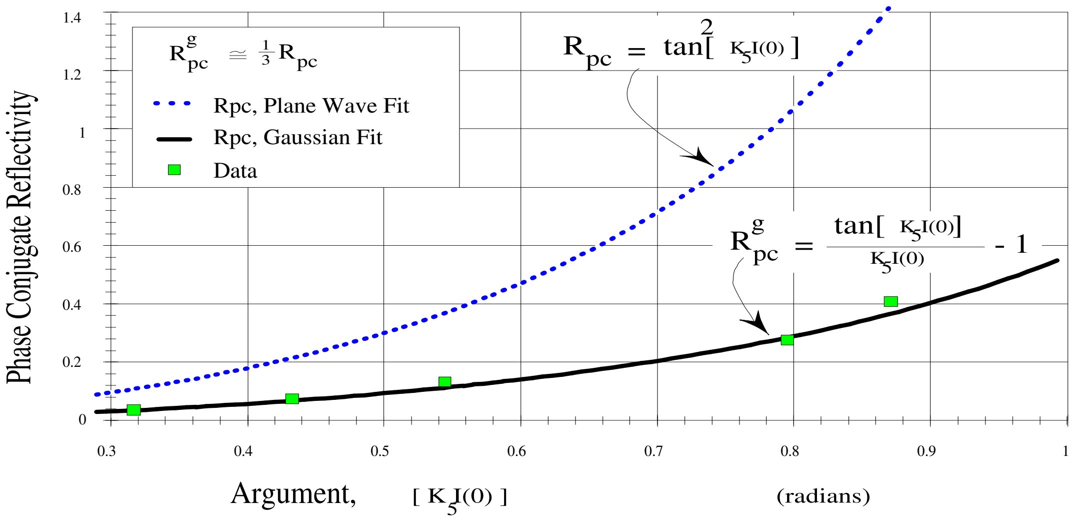

Figure 4: Measured backward DFWM phase-conjugate reflectivities in CS_2 as a function of pump-beam power. The upper line is a theoretical fit using plane-wave theory, whereas the lower line is the theoretical fit in which the Gaussian spatial profile of the pump beam is taken into account.

In the low gain regime, the new analytical solutions for R_{pc} and T_{pc} should provide better agreement between theory and experiment, and also improve accuracy of $\chi^{(3)}$ measurements taken via FWM[17] by at least a factor of $\sqrt{3}$. This should be especially apparent when comparing to Z-scan measurements of $\chi^{(3)}$[18] which account for the Gaussian nature of the laser beam.

3 EXPERIMENTAL SETUP

Figure 5 is a schematic of the experimental setup. The output of a Q-switched and mode-locked Nd:YAG laser is divided into pump and signal beams. At a repetition rate of 1.1 kHz the Q-switch envelope is $\approx$ 270 ns in duration and the mode-locked pulses underneath the Q-switch envelope are $\approx$ 120 ps, repeating every 10 ns, generating a peak power of up to 200 kW. The optical isolator polarizes the beam and prevents destabilizing backreflections. Beam intensity is adjusted by the half and quarter-wave plate combination (QWP1 and HWP2). The probe input is generated from a portion of the main beam reflected from beam splitters BS1 and subsequently BS2. Pump intensity is adjusted by (HWP2), and prisms (PR1 and PR2) are used to adjust the path lengths of the various beams incident on the sample to within a few millimeters to ensure that the various mode-locked pulses enter simultaneously. To minimize Fresnel losses and to improve spatial overlap within the medium, we use a Brewster configuration.

Pump and probe beams are incident on the 2 mm thick CdTe single crystal[24] at Brewster's angle with an angular separation of $\theta \simeq 1^o$ and $\phi = 0^o$, (see Figure 1). In this configuration, the measured optical transmission through the sample was better than 97% corresponding to a linear (intensity) loss coefficient $\alpha < 0.2\,\mathrm{cm}^{-1}$. With an intensity radius of 60 μm (e^{-1} point), we obtain pump intensities exceeding 500 MW/cm^2.

Two InGaAs photodiode detectors, D1 and D4, perform the detection of the forward FWM outputs as follows. Detector D4 measures the amplified probe during FWM and the probe input when the pump is blocked. The forward conjugate is measured at D1. The detectors are connected so that their photo-currents subtract when light is incident on both detectors, generating the difference signal. Since the amount gained by the probe and forward conjugate should be equivalent, the difference signal should equal the probe input for FWM in a lossless material. This detection arrangement provides a convenient method of monitoring the individual FWM outputs and the difference.

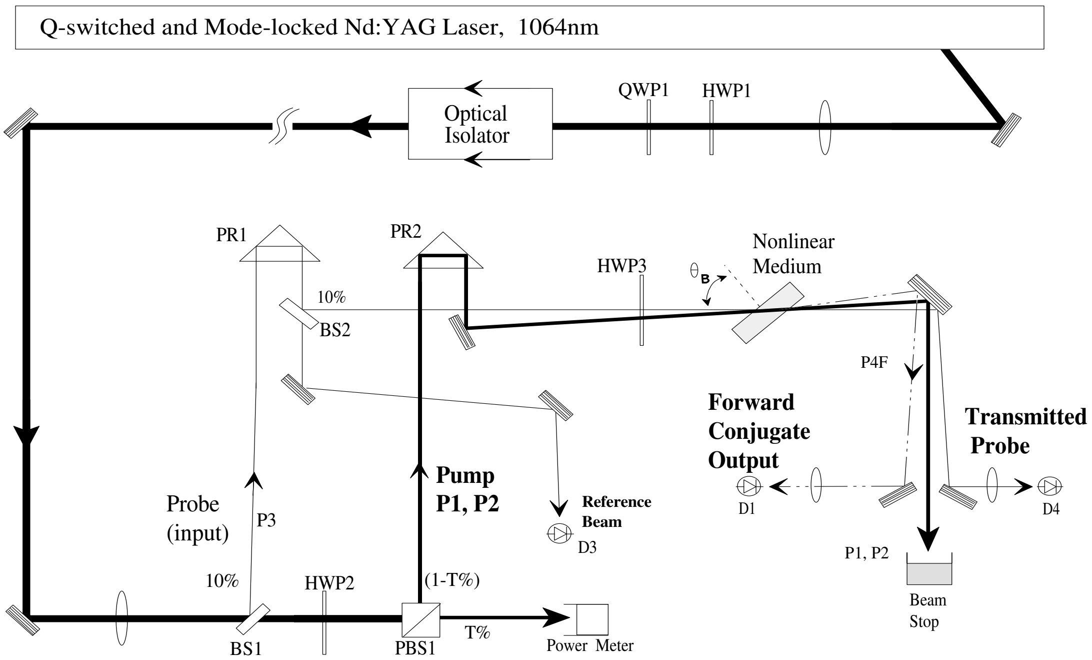

Figure 5: Experimental setup for measuring gain response of reflected conjugate and transmitted probe beams in forward DFWM.

4 EXPERIMENTAL RESULTS

Agreement of experimental data with the $T_{\rm pc} - R_{\rm pc} = 1$ relationship of Eq. 4 is shown in Figures 6 and 7, for a maximum conjugate reflectivity of 164%. As expected, the difference signal is approximately equal to the probe over the duration of the Q-switch pulse.

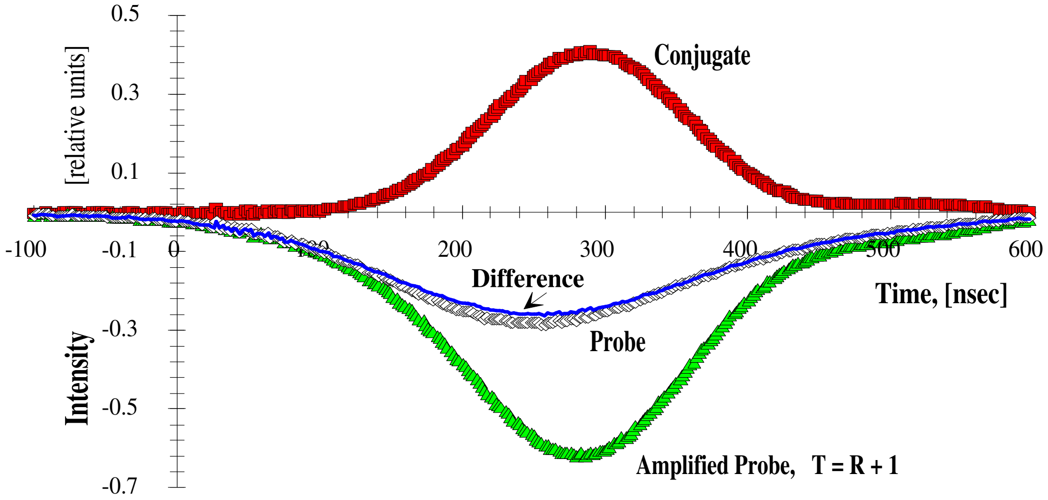

Figure 6: Amplified transmission and phase-conjugation data from forward FWM in 2 mm CdTe.

By dividing the conjugate and amplified probe Q-switch data by the probe input, $T_{\rm pc}$ and $R_{\rm pc}$ coefficients are obtained as functions of time. Subtracting the two demonstrates experimental agreement with Eq. 4 as shown in Figure 7. Deviation from the $T_{\rm pc} - R_{\rm pc} = 1$ line during high gains is probably due to nonlinear (two-photon) absorption. These deleterious effects can be prevented by working at wavelengths below half band gap,[19–21] where two-photon absorption is prohibited.

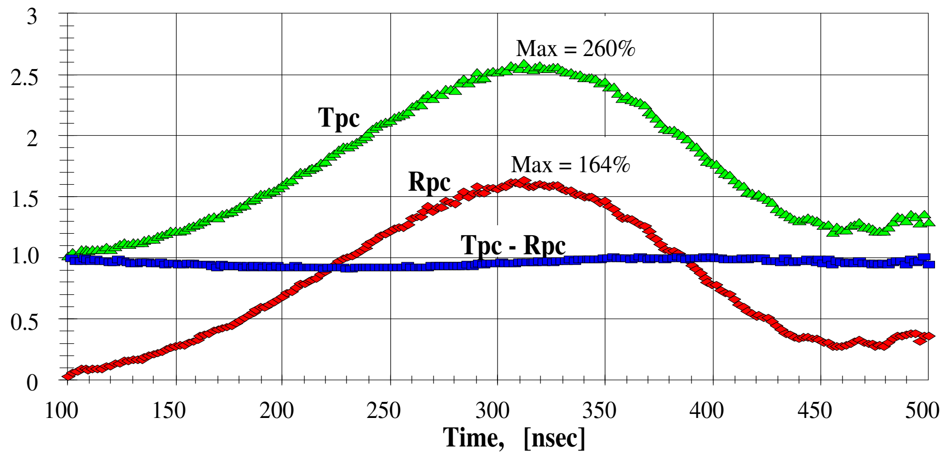

Figure 7: FWM reflection and transmission coefficients, $R_{\rm pc} = |\frac{conjugate}{probe}|$ and $T_{\rm pc} = |\frac{amplified\ probe}{probe}|$, confirming the $T_{\rm pc} - R_{\rm pc} = 1$ relationship shown over the duration of the Q-switch pulse.

Amplification of mode-locked pulses under the Q-switch envelope is shown in Figure 8. Even in the fast regime, the gain in the probe (i.e., the difference between amplified probe and probe input signals) closely matches the conjugate trace maintaining the $T_{pc} = R_{pc} + 1$ relationship. Note that the peak of the probe is between 3 and 5 mode-locked pulses (30-50nsec) before the peak of the conjugate. Although a nonlinear response time of 1 ns for CdTe was reported in reference 22, the time-shifted conjugate peak relative to the probe input implies the CdTe nonlinear response time is greater than the 10 ns between pulses in order for the contribution of earlier pulses to build up in this delayed manner.

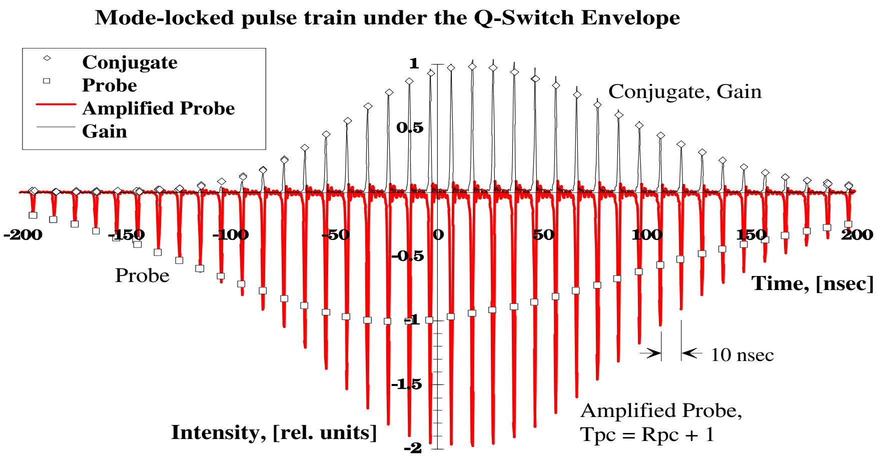

Figure 8: Amplified transmission and phase-conjugation of 100psec mode-locked pulses via forward FWM in CdTe. Positive conjugate, negative probe and amplified probe signals are shown as a function of time. Probe gain is calculated from the difference between the probe and amplified probe signals. The train of 40 mode-locked pulses under the Q-switch envelope are seen to be 10 nsec apart.

The time-dependent effect is emphasized in the plot of phase-conjugate reflectivity verses pump intensity (R_{pc} -vs- I_{pump}) and results in the hysteresis between the rising and falling edges of the pump shown in Figure 9. While the data is quadratic over the lower portion of the curves as expected from Eq. 8, it is difficult to make comparisons between the time-independent theory and time-dependent data.

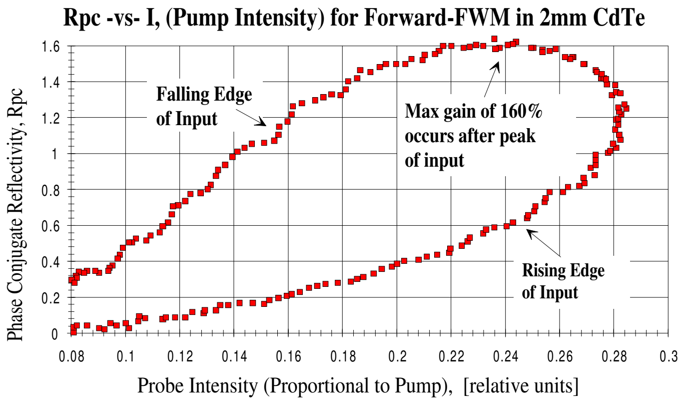

Figure 9: Measured forward DFWM phase-conjugate reflectivities as a function of pump beam power. The apparent bi-stability is due to the time dependent response of the material, which causes the hysteresis between the rising and falling edges of the pump.

The FWM process can amplify both transmitted and reflected waves of arbitrary complexity.[1] Since forward FWM can be nearly phase-matched over numerous propagation vectors satisfying $\mathbf{k}_4 \simeq \mathbf{k}_1+\mathbf{k}_2-\mathbf{k}_3$, multiple signal inputs distinguished by $\mathbf{k}$, can theoretically be amplified and copied by the process that we have demonstrated. By representing an image by N signals, FWM could be used to amplify each of the signals simultaneously as well as generate an amplified copy of each as illustrated in Figure 10. In the laboratory, a two-signal forward FWM experiment was performed and conjugate outputs for both input signals were observed as expected. Future experiments are planned to characterize the multi-FWM process further and to determine if a multi-channel amplifier can in fact be implemented.

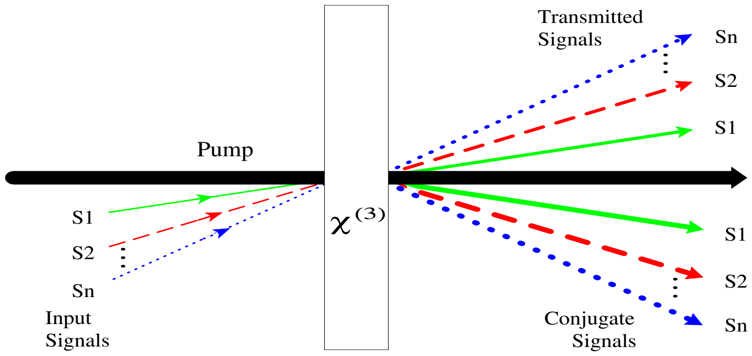

Figure 10: Optical splitting with gain via forward FWM.

5 CONCLUSION

In conclusion we have experimentally investigated degenerate FWM in CdTe, and have measured gain in both transmitted probe and reflected phase-conjugate outputs, in accordance with the gain relationship of $T_{\rm pc} = 1+R_{\rm pc}$. Since phase-matching can occur over a wide range of incident angles, it is possible to use this process for image amplification and duplication, or equivalently, the simultaneous amplification and splitting of multiple input signals. With this capacity to perform *optical splitting with gain*, efficient FWM processes could have a profound impact on the local distribution of information where large information fan-out is required.

This work was supported in part by the National Science Foundation. We also acknowledge support from ISP Inc.[24] for providing low loss CdTe single crystals.

6 REFERENCES

[1] A. Yariv and D. M. Pepper. Amplified reflection, phase conjugation and oscillation in degenerate four-wave mixing. *Optics Letters*, 1(1):16–18, July 1977.

[2] D. M. Pepper, D. Fekete, and A. Yariv. Observation of amplified phase-conjugate reflection and optical parametric oscillation by degenerate four-wave mixing in a transparent medium. *Applied Physics Letters*, 33:41–44, July 1978.

[3] R. A. Fisher, editor. *Optical Phase Conjugation*. Academic Press, New York and NY, 1983.

[4] M. Gower and D. Proch. *Optical Phase Conjugation*. Springer-Verlag, New York, 1993.

[5] H. P. Yuen and J. H. Shapiro. Generation and detection of two-photon coherent states in degenerate four-wave mixing. *Optics Letters*, 4(10):334–336, Oct. 1979.

[6] P. Kumar and J. H. Shapiro. Squeezed-state generation via forward degenerate four-wave mixing. *Physical Review A*, 30(3):1568–1571, Sept. 1984.

[7] R. W. Boyd. *Nonlinear Optics.* Academic Press, New York, 1992.

[8] M. Cronin-Golomb, B. Fischer, J. Nilsen, J. White, and A. Yariv. Laser with dynamic holographic intracavity distortion correction capability. *Applied Physics Letters*, 41:220, 1982.

[9] R. D. Li, P. Kumar, W. L. Kath, and J. N. Kutz. Combating dispersion with parametric amplifiers. *IEEE Photonics Technology Letters*, 5(6), June 1993.

[10] R. M. Jopson, A. H. Gnauck, and R. M. Derosier. Compensation of of fibre chromatic dispersion by spectral inversion. *Electronic Letters*, 29(7), April. 1993.

[11] S. Watanabe, T. Naito, and T. Chikama. Compensation of chromatic dispersion in a single-mode fiber by optical phase conjugation. *IEEE Photonics Technology Letters*, 5(1), Jan. 1993.

[12] J. B. Norman. Phase-conjugate michelson interferometers for all-optical image processing and computing. *American Jounal of Physics*, 60(3):212, March 1992.

[13] S. Sukushima and T. Kurokawa. Parallel interconnection through an optical fiber using phase conjugation mirror acceptable for optical data pattern. *IEEE Journal of Quantum Electronics*, 29(2), Feb. 1993.

[14] S. Anderson. Optical phase conjugation corrects fiber-induced beam distortion. *Laser Focus World*, 30(11), Nov. 1994.

[15] M. Kauranen and R. W. Boyd. Correlated amplification of light. *Physical Review A*, 47(5):4297–4301, May 1993.

[16] C. Kim, R. D. Li, and P. Kumar. Deamplification response of a traveling-wave phase-sensitive optical parametric amplifier. *Optics Letters*, 19:132–134, Jan 1994.

[17] A. A. Said, D. J. Hagan, J. Young, and E. W. Van Stryland. Degenerate four-wave mixing measurements of high order nonlinearities in semiconductors. *IEEE Journal of Quantum Electronics*, 27(10), Oct. 1991.

[18] M. Sheik-Bahae, A. A. Said, T. H. Wei, D. J. Hagan, and E. W. Van Stryland. Sensitive measurement of optical nonlinearities using a single beam. *IEEE Journal of Quantum Electronics*, 26(4), April 1990.

[19] M. K. Udo, X. Zhang, and S. T. Ho. Theoretical and experimental investigations of sqeeze-state generation in χ^3 semiconductor waveguides. In *International Quantum Electronics Confence Summary.* OSA and IEEE-LEOS, May 1994.

[20] R. E. Slusher, S. L. McCall, A. Mysyrowicz, S. Schmitt-Rink, and K. Tai. *Nonlinear Optics of Organics and Semiconductors.* Springer-Verlag, Berlin, 1989.

[21] A. M. Fox, B. Huttner, and J. F. Ryan. Evaluation of GaAsAlGaAs MQW waveguides and bulk ZnSe for pulsed squeezed-light generation. In *OSA Annual Meeting Abstract Summary.* Optical Society of America, Oct 1994.

[22] V. Kremenitskii, S. Odoulov, and M. Soskin. Dynamic gratings in cadmium telluride. *Phyicss Status Solidi*, 51:K63–K66, 1979.

[23] D. O. Caplan and P. Kumar. Degenerate four-wave mixing noise measurements in semiconductors. In *OSA Annual Meeting Abstract Summary.* Optical Society of America, Oct 1994.

[24] Internation Science Products,Tarrytown, NY. *Source of CdTe single crystals.*